Radiative lifetimes and collisional deactivation cross sections of the $5d6p$ states of laser-ablated Ba in He gas

Yukari Matsuo, Takashi Nakajima,* Tohru Kobayashi, and Michio Takami
The Institute of Physical and Chemical Research (RIKEN), 2-1 Hirosawa, Wako, Saitama 351-0198, Japan
(Received 5 June 1998)

We have measured radiative lifetimes and collisional deactivation cross sections of the $5d6p$ excited states of Ba atoms in He buffer gas. Barium atoms are produced by laser ablation of a solid Ba sample, whereby populating the $6s5d\,^3D_J$ metastable states about 0.1–1% of the total population. The $5d6p\,^{1,3}P^o$, $^{1,3}D^o$, and $^{1,3}F^\circ$ states, most of which are not accessible from the ground state by single-photon transition, are excited from the metastable states by a laser, and radiative lifetimes as well as collisional deactivation cross sections are determined from the decay rates of the laser-induced fluorescence. Radiative lifetimes of the $5d6p\,^3P^o_J$, $^3D^o_J$, and $^3F^o_J$ states do not depend on J, indicating the validity of LS coupling scheme. Collisional deactivation cross sections by He are in the range of 5–20 Å^2 for the $5d6p\,^3D^o_J$, $^1D^o_2$, and $^3F^o_{3,4}$ states, whereas those for the $5d6p\,^3P^o_J$, $^1P^o_1$, $^3F^o_2$, and $^1F^o_3$ states are less than 1.5 Å^2 in the He pressure range of 60–400 Pa. Among $5d6p$ manifolds, the $5d^2\,^3P_2$ state is populated by the collisional deactivation from the laser-excited $5d6p\,^3D^o_1$ state, leading to the sensitized fluorescence from $5d^2\,^3P_2$. Radiative lifetime and collisional deactivation cross section of the $5d^2\,^3P_2$ state are also determined from the decay rates of the sensitized fluorescence. [S1050-2947(99)09403-2]

PACS number(s): 34.50.−s, 33.50.−j, 32.70.Cs

I. INTRODUCTION

Radiative lifetimes and collisional deactivation cross sections of atomic excited states are fundamental quantities and correlated to atomic structures and interaction potentials. Measurement of radiative lifetimes and branching ratios is very important, since it leads to the precise determination of transition probabilities.

Study of the transition probabilities of Ba has a long history [1]. Oscillator strengths and radiative lifetimes of principal series [2–4] and Rydberg series [5,6] have been reported. Although the transition probabilities of the moderately excited states ($\lesssim$30 000 cm^{-1}) of Ba have been extensively studied in discharge cells [7–11], *direct* lifetime measurements of the excited states, which lack significant oscillator strengths from the ground state, are limited to few cases. In order to measure the lifetimes of such excited states, two methods have been employed so far. One is to excite atoms from metastable states produced by electron bombardment or discharge [12,13], and the other is to populate excited states collisionally from the states initially pumped by a laser [14]. For the collisional population transfer of Ba, collisions with rare gas atoms have been studied in the past decade. Such studies are mainly focused on the states below $6s6p\,^1P^o_1$ [15–22], except the one on population transfer among Rydberg states [23].

One of the limitations to investigate atomic excited states arises from the fact that there are relatively few excited states, which are accessible by single-photon excitation from the ground state. Even for moderately excited states such as the $5d6p$ states of Ba, the majority of the states cannot be reached from the ground state because the transitions to these states are electric dipole-forbidden. Thus, the use of metastable states instead of the ground state should be helpful to increase the number of accessible states. For example, all the $5d6p$ states of Ba can be easily excited if the $6s5d\,^3D_J$ metastable states are produced since the excitation process is essentially a single-electron transition $6p \leftarrow 6s$ (see Fig. 1). Recently, we have used the laser-ablation technique to produce atoms and molecules of neutral and ionic species [24–28] for the study of collision and reaction dynamics of produced atoms and molecules. Right after the ablation, laser-induced plasma contains highly excited atoms and ions.

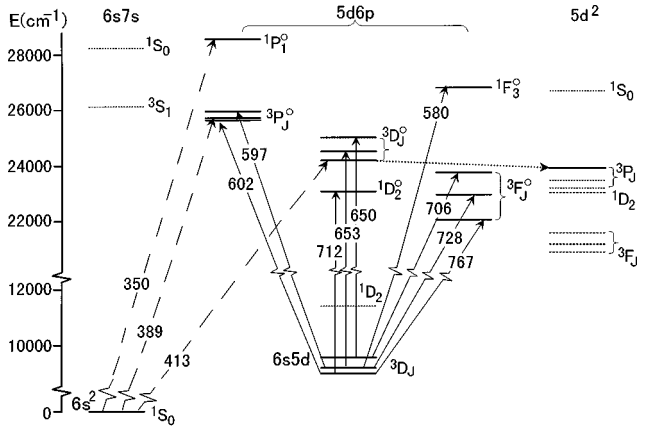

FIG. 1. Relevant energy-level diagram of Ba below 30 000 cm^{-1}. States from which fluorescence is observed are depicted with thick solid lines. Solid arrows represent optical excitation from the $6s5d\,^3D_J$ metastable states and broken arrows from the $6s^2\,^3S_0$ ground state. The dotted arrow represents collisional population transfer process observed in this paper. For all fine structures, J increases from a lower to a higher level. Wavelengths of the excited transitions are shown in nm.

*Present address: Institute of Advanced Energy, Kyoto University, Uji, Kyoto 611-0011, Japan.

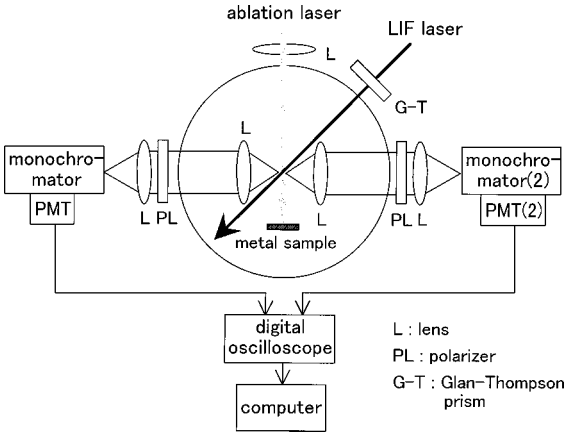

FIG. 2. An experimental setup for the LIF study of laser-ablated atoms. Second monochromator and photomultiplier tube (PMT) are used for simultaneous observation of LIF and sensitized fluorescence.

During the thermalization process in buffer gas, atoms are populated in metastable states. This indicates the feasibility of applying a laser-ablation technique for the creation of translationally thermalized metastable atoms.

One important advantage of producing atoms by laser ablation is that the temperature of atoms can be controlled by changing the buffer-gas temperature, because translational temperature of ablated atoms is thermarized by collisions with buffer gas within several tens of μs [26]. Thus the collisional process can be studied in a wide range of temperature, in particular at low temperature $\sim$10 K [28]. We note that the Ba $6s5d$ metastable states can also be populated by optical pumping through the $6s6p\,^3P_1^o$ state. Population transfer and pressure broadening among the $6s5d$ metastable states have been studied by this method [19–22]. However, the temperature is limited to be high (700–1100 K) because a heat pipe oven has been used to vaporize Ba atoms. Even higher temperature would be required to vaporize refractory metals using ovens.

In this paper, we report the measurement of radiative lifetimes and collisional deactivation cross sections of the Ba $5d6p$ doubly excited states in He gas at room temperature through laser-induced fluorescence (LIF), pumped *from the* $6s5d$ *metastable states* which are produced by laser ablation. In addition, we have found that the $5d^2\,^3P_2$ state, which is not directly excited by a laser, is populated by collisional deactivation process from the laser-excited $5d6p\,^3D_1^o$ state, and observed sensitized fluorescence from $5d^2\,^3P_2$ (see Fig. 1). This method also serves as a powerful tool to study radiative and collisional decay of the states that cannot be reached from the ground state by single-photon excitation [23].

II. EXPERIMENT

The experimental setup shown in Fig. 2 is similar to the one used in our previous work on collisional depolarization [27]. A solid Ba sample is placed 1 cm off the center of a vacuum chamber whose background pressure is maintained at about 1×10^{-5} Pa by two turbo molecular pumps in series. During the measurement of collisional deactivation processes, 60–400 Pa of He gas (research grade, 99.9999%) is introduced into the chamber through a variable leak valve. Helium pressure is monitored by a capacitance manometer (MKS Baratron 626A) with an accuracy of 10 Pa. Laser ablation is performed with a fundamental frequency output of a Nd:YAG laser (Lumonics Mini-Q, 1.06 μm, 8 ns pulse duration, 10 Hz) that irradiates the Ba sample with normal incidence to the sample surface and produces laser-ablation plasma containing vaporized atoms and ions. The output power of 20 mJ/pulse is moderately focused onto the sample with a 1-m focal length lens, which is placed at 0.5 m apart from the sample, leading to the energy density of $\sim1\times10^8$ W cm^{-2}, which produces typically 10^{12} atoms per pulse. The delay time between the ablation and LIF excitation laser pulses is set to 50 μs in vacuum condition and 500 μs when He buffer gas is introduced. Since the ablation plasma emission lasts only for 20–30 μs in vacuum and for 40–50 μs in He buffer gas, the LIF detection is not influenced by the emission from plasma plume. The number of atoms in the detection region decreases to about 1/50 of the initial value 500 μs after the ablation. The output of a pulsed dye laser (Lambda Physik FL3002, 15-ns pulse duration) pumped by a XeCl excimer laser (Lambda Physik MSC103) is introduced into the vacuum chamber for the excitation of $6s5d\,^3D_J$ metastable Ba atoms to the $5d6p$ excited states (see Fig. 1). Fractional population of the $6s5d\,^3D_J$ metastable states is approximately 0.1–1% of the total population, which is estimated from the relative intensity of LIF signals originated from the ground and metastable states in He buffer gas together with the excitation laser intensities and the relevant oscillator strengths. Since the lack of buffer gas cooling process in vacuum condition leads to smaller population of the metastable states ($\sim$0.01%) in the detection region, shorter delay time is chosen for the measurement in vacuum to maintain sufficient signal-to-noise ratio. Polarization of the excitation laser beam is fixed with a Glan-Thompson prism and the output power is attenuated to 20–30 nJ per pulse by neutral-density filters in order to avoid saturation of transitions, which would distort the time profile of the LIF signal. A polarizer is set to the magic angle and placed in front of the monochromator to compensate polarization effect. The LIF signal is detected by a photomultiplier tube (Hamamatsu-Photonics R955) through a 0.25 m monochromator (JASCO CT25). Time-resolved fluorescence signals are amplified by a fast preamplifier and sent to a digital oscilloscope (Tektronix TDS 520A) with a 200 ps time resolution. The signals are averaged over 2000 shots and stored in a computer for further data processing. For the observation of sensitized fluorescence, another set of optical detection system with a monochromator, a photo-multiplier tube (Hamamatsu-Photonics R636-10), a fast preamplifier, and optics are used for the simultaneous observation of the LIF signal from the state initially excited by the dye laser and the sensitized fluorescence signal from collisionally populated states.

III. DATA ANALYSIS

In order to obtain the radiative lifetimes and collisional deactivation cross sections from LIF and sensitized fluorescence, we employ a set of rate equations based on a kinetic

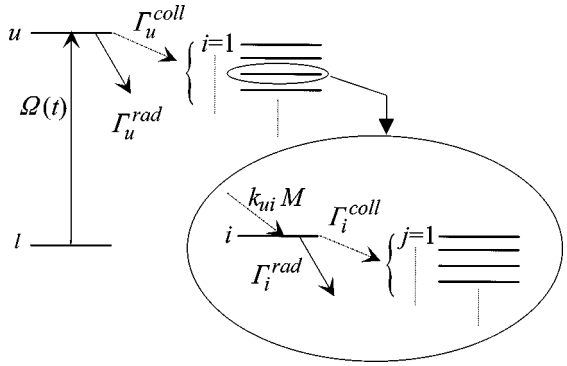

FIG. 3. Relevant energy levels described in Eqs. (1)–(5).

model. A simplified energy level diagram is shown in Fig. 3. Atoms in the lower state l are excited by a pump laser to the upper state u with a pumping rate $\Omega(t)$; then the upper state is depopulated either radiatively to the lower states or collisionally to the nearby states i. Note that what can be determined from the experiment is not a radiative or collisional decay rate but rather the total decay rate of both processes. Rate equations for the populations of the upper and the lower states N_u and N_l are given as

$$\dot{N}_l = -\Omega(t)(N_l - N_u) + R\Gamma_u^{rad} N_u - \Gamma_l N_l, \tag{1}$$

$$\dot{N}_u = \Omega(t)(N_l - N_u) - \left(\Gamma_u^{rad} + \sum_{i\neq u} k_{ui} M\right) N_u + \sum_{i\neq u} k_{iu} M N_i, \tag{2}$$

where Γ_u^{rad} is the radiative decay rate of u and k_{ui} is the collisional population transfer rate constant from u to i under buffer-gas density M. The back-transfer rate constant from i to u is denoted as k_{iu} and the population of the ith state as N_i. In our experimental scheme, l represents either the ground state or one of the $6s5d$ metastable states, whereas u represents one of the $5d6p$ excited states. In Eq. (1), R represents a fraction of the effective repopulation due to the radiative decay of the upper state. In reality, R does not affect the time profile of the LIF signal in the weak pumping regime. For the $6s5d$ metastable state, the lower state l depopulates with the rate Γ_l due to radiative decay and collisional deactivation. It has turned out, however, that these processes are very slow [22,29] in our experimental condition so that Γ_l is ignored in the analysis. Depopulation processes due to collisions with impurities are not taken into account in this analysis because collisions with He are considered to dominate the total depopulation processes. This is based on the following consideration: the impurities are mostly nitrogen molecules. Collisional cross sections with N_2 for the states of Ba studied in the present paper are not available in literature. Cross sections of Ba^+ metastable states with N_2 are reported to be two orders of magnitude larger than those with He [30]. If this relation still holds for the present system, N_2 impurity of 0.0001% will result in additional 0.01% of the cross sections with He. Note that this number may be an overestimation since the effect of the impurities are usually smaller for Ba than for Ba^+. The last term of Eq. (2) corresponds to the secondary collision processes, which can be neglected for low buffer-gas density, because the radiative decay from the state i occurs before the collisional population transfer takes place from the same state [23]. Collisional deactivation rate of the state u can be defined as

$$\Gamma_u^{coll} = \sum_{i\neq u} k_{ui} M, \tag{3}$$

which is the sum over the outgoing transfer rates.

The population N_i for the state i, populated by collisional transfer from the laser-excited state u, is described by

$$\dot{N}_i = k_{ui} M N_u - \left(\Gamma_i^{rad} + \sum_{j\neq i} k_{ij} M\right) N_i + \sum_{j\neq i} k_{ji} M N_j, \tag{4}$$

where Γ_i^{rad} is a radiative decay rate from i, k_{ij} and k_{ji} are the collisional population transfer rate constants from i to j and vice versa, and N_j is the population of the jth state. The last term of Eq. (4), which describes the secondary collision processes, is also neglected for low buffer-gas density. Collisional deactivation rate of the state i can be defined as

$$\Gamma_i^{coll} = \sum_{j\neq i} k_{ij} M. \tag{5}$$

Once the pumping function $\Omega(t)$ and all the decay rates Γ's are given, the time evolution of the LIF (for the laser-excited state u) and sensitized fluorescence (for the collisionally populated state i) can be calculated from Eqs. (1)–(5). Now, we determine the pumping function $\Omega(t)$ by fitting scattered light of the dye laser to a combination of Gaussian functions, which represents the convolution of the temporal laser-pulse profile and an instrumental function. Then, we calculate the time evolution of the fluorescence signals, which is virtually the convolution of the pumping function and exponential decay, and fit the time profiles of the LIF and the sensitized fluorescence with adjustable parameters $\Gamma_u (= \Gamma_u^{rad} + \Gamma_u^{coll})$ for u and $\Gamma_i (= \Gamma_i^{rad} + \Gamma_i^{coll})$ for i. After going through iteration loops of least-squares fitting, the depopulation rates Γ_u and Γ_i are determined. Note that each state-to-state transfer rate constant k_{ui} cannot be determined from the time profile of the fluorescence signal when there are more than one collisional decay channels. In other words, time profile of the sensitized fluorescence is characterized only by the total depopulation rates Γ_u and Γ_i [14].

IV. RESULTS AND DISCUSSION

Representative time profiles of LIF from Ba $5d6p$ excited states and fitted curves are depicted in Fig. 4. In our previous work on Ba-He system [27], the $^3D_1^o$ state has shown relatively fast collisional deactivation among the $5d6p\,J=1$ states, i.e., $^1P_1^o$, $^3P_1^o$, and $^3D_1^o$. One of the states collisionally populated from $5d6p\,^3D_1^o$ is found to be the $5d^2\,^3P_2$ state, from which sensitized fluorescence is observed at 886 nm. In Fig. 5, we show examples of experimental data and fitted curves for the sensitized fluorescence together with LIF from the laser-excited $5d6p\,^3D_1^o$ state. The total depopulation rates Γ_u and Γ_i are obtained by the procedure described in Sec. III. The fact that the decay profiles of LIF and sensitized fluorescence signals are well described

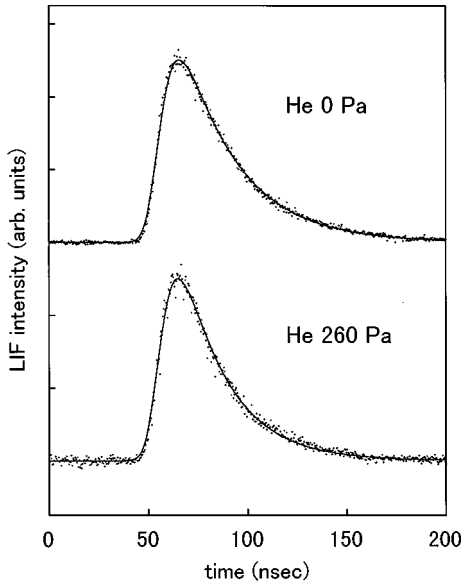

FIG. 4. Experimental time profiles of the LIF signal and fitted curves for the $5d6p\ ^3F_4^o$ state with and without He gas.

by a single decay rate indicates that our approximation, which neglects secondary collision processes and radiation trapping effect, is valid. Lifetime measurements by time-resolved fluorescence inherently suffer from radiation trapping. The density of ablated atoms is difficult to estimate since it varies in time and space after the ablation. In order to check the effect of radiation trapping, we have carried out lifetime measurements of the $6s6p\ ^1P_1^o$ state excited from the $6s^2\ ^1S_0$ ground state (553 nm) at different delay times, or equivalently at different density of atoms. This transition line is considered to give the most serious radiation trapping effect due to short radiative lifetime (8.37 ns [2]) and nearly closed transition cycle between the ground and the excited states. We have found that lifetimes measured after the delay

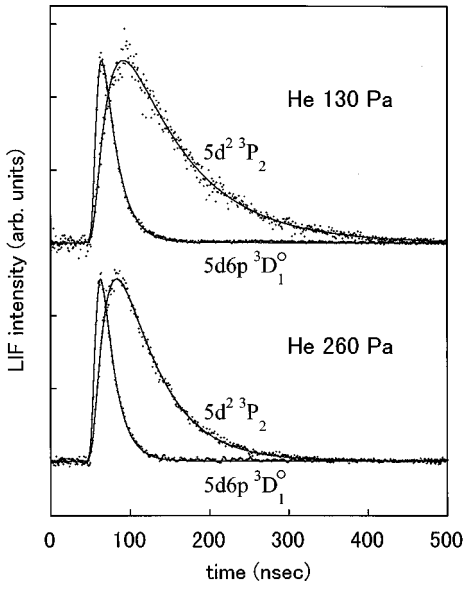

FIG. 5. Experimental time profiles of the sensitized fluorescence signal from the $5d^2\ ^3P_2$ state with He gas at 130 and 260 Pa. The LIF signal from the laser-excited $5d6p\ ^3D_1^o$ state is also shown. Relative intensities are not to scale. Solid lines are fitted curves.

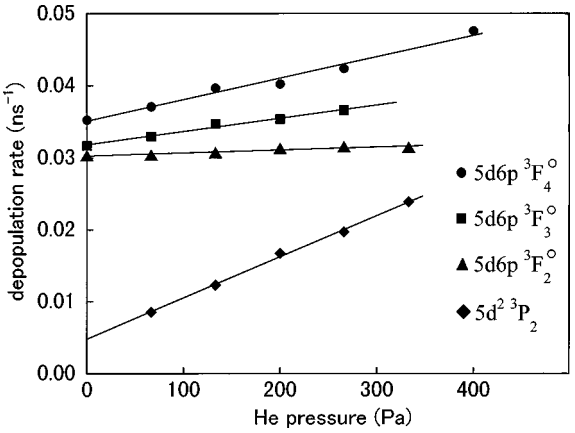

FIG. 6. Total depopulation rates of the $5d6p\ ^3F_J^o$ and $5d^2\ ^3P_2$ states as a function of He pressure.

time longer than 400 μs agree with reported values within 1% in our experimental condition. For the emission lines to the metastable states, radiation trapping effect is even less than those to the ground state, because number densities of the metastable atoms are less than 1% of the density of the ground-state atoms.

Pressure dependence of the total depopulation rates of the $5d6p$ states is shown in Fig. 6. The slope and the intercept with vertical axis correspond to the deactivation rate constant and the radiative decay rate, respectively. Despite a large difference of the delay times between ablation and LIF lasers for the measurements in vacuum and He buffer gas, the measured radiative decay rates in vacuum agree within 1% with those obtained by extrapolating the data in He buffer-gas condition. Since the detection region is about 1 cm from the Ba sample surface, the atoms excited with 50 and 500 μs delay times are estimated to have a mean diffusion speed of 200 and 20 m s^{-1}, respectively, along the direction of the surface normal if they come directly from the sample surface to the region. These values are, however, comparable to and well below 250 m s^{-1}, the thermal velocity of Ba at room temperature, and therefore Ba atoms are safely considered to have been thermalized at the region. Because of the long lifetimes of the $6s5d\ ^3D_J$ metastable states ($\sim$60 s) [29] and efficient cooling by He buffer gas, a sufficient number of metastable atoms are present even 500 μs after the ablation. On the other hand, 100 μs after the ablation in a vacuum, metastable atoms are not found in the detection region due to nearly collision-free expansion of ablated atoms after the plasma plume disappers. Therefore, we set the delay time to 50 μs in a vacuum experiment, as mentioned in Sec. II, to maintain reasonable LIF signal-to-noise ratio. Good agreement between radiative decay rates measured in a vacuum and the decay rates determined from experiments in He buffer gas indicates that a relatively high translational temperature of Ba atoms in a vacuum experiment does not degrade the reliability of measured radiative decay rates. Figure 6 also shows pressure dependence of the total depopulation rates of the collisionally populated $5d^2\ ^3P_2$ state. No cascade emission from the $5d^2\ ^3P_2$ state is observed in a vacuum. The radiative decay rate is determined by extrapolating the data of sensitized fluorescence versus He buffer-gas pressure.

The radiative decay rates are easily converted into radia-

TABLE I. Ba(I) radiative lifetimes and collisional deactivation cross sections with He at 295 K.

	Radiative lifetime (ns)			Deactivation cross section (Å^2)
Ba state	This paper [a]	Lifetime measurement	Emission intensity	This paper [a]
$5d6p\ ^1P_1^o$	12.4±0.9	12.4±0.9[b]		<1
$5d6p\ ^3P_0^o$	12.1±0.5			<1
$5d6p\ ^3P_1^o$	12.0±0.7	11.7±0.9[b]		<1
$5d6p\ ^3P_2^o$	12.4±0.7		13±2 [e]	<1
$5d6p\ ^1D_2^o$	25.8±0.8		32±5 [f]	16.9±1.0
$5d6p\ ^3D_1^o$	17.6±0.9	17.0±0.5[b]		12.3±0.5
$5d6p\ ^3D_2^o$	17.5±0.6		18±3 [f]	5.4±0.4
$5d6p\ ^3D_3^o$	17.3±0.6	10.2±1.5[c]		4.9±0.7
$5d6p\ ^1F_3^o$	45.0±2.3	44.5±1.8[d]		1.2±0.4
$5d6p\ ^3F_2^o$	32.3±0.8		34±6 [f]	1.3±0.5
$5d6p\ ^3F_3^o$	30.8±1.2		30±5 [f]	6.0±0.9
$5d6p\ ^3F_4^o$	27.9±0.7			10.0±0.9
$5d^2\ ^3P_2$	207±27			18.4±1.1

[a]Estimated errors are two standard deviations.
[b]Reference [3].
[c]Reference [13].
[d]Reference [12].
[e]Reference [9].
[f]Reference [8].

tive lifetimes. As for the collisional deactivation rates, they are converted to the velocity-averaged cross sections by using the relation

$$\sigma^{coll}=\frac{\Gamma^{coll}}{\bar{v}M}, \tag{6}$$

where $\bar{v}$ is the average Ba-He relative velocity given by $\bar{v}=\sqrt{8k_BT/\pi\mu}$ with the Boltzmann constant k_B and the reduced mass of the Ba-He system given by μ. Obtained radiative lifetimes and deactivation cross sections in He gas at 295 K are summarized in Table I. The values obtained by radiative lifetime measurements (Hanle effect [2,3,13] and delayed coincidence method [12]) and those calculated from relative emission intensity using Ladenburg method [8,9,31] are also listed in Table I for comparison. It can be seen that our results of the lifetime measurement agree reasonably well with previously reported values. Note that the lifetimes of the most of $J\neq 1$ states, namely, the states that cannot be reached from the ground state by electric dipole-allowed transitions, have not been directly measured so far. Niggli and Huber have given lifetimes of these states by measuring the relative emission intensity of two lines that share common lower state but have different upper states, one of which has a known lifetime while the other does not [8,9]. These calculated lifetimes appear to be in good agreement with our results within estimated errors although their uncertainty range is large. The large uncertainty in their values is partly caused by the ambiguity of more than one possible common lower states, which sometimes give scattered results. The measured radiative lifetimes show strong dependence on orbital angular momentum L and spin multiplicity $2S+1$, but not on total angular momentum J. This result indicates the validity of LS coupling for the $5d6p$ states.

The determined collisional deactivation cross sections show more complicated dependence on L, S, and J. Very small cross sections are obtained for the $5d6p\ ^1P_1^o$, $^3P_J^o$, $^1F_3^o$, and $^3F_2^o$ states while the $5d6p\ ^1D_2^o$, $^3F_{3,4}^o$, and $5d^2\ ^3P_2$ states give cross sections of the order of 10 Å^2. In our pressure range of He buffer gas, where the secondary collision is negligible, a deactivation cross section below 1 Å^2 cannot be measured with reasonable accuracy. Naturally, collisional population transfer processes can be interpreted by atom-atom potential curves and energy differences between transferring states. Unfortunately, no potential curves are available for the Ba($5d6p$)-He system except for the lowest $5d6p\ ^3F_2^o$ state [32], so that we cannot discuss the state-specific collisional processes. Thus we speculate the propensity of the population transfer by comparing the present result with previously reported results for Ba-rare gas systems. First, our experimental results suggest that intramultiplet mixing (fine-structure mixing) is small for the $5d6p\ ^3P_J^o$ states. This is in agreement with the general trend of weaker fine-structure mixing in $6s6p\ ^3P_J^o$ and $6s5d\ ^3D_J$ than intermultiplet mixing [16,22]. In our experiment, both $5d6p\ ^1P_1^o$ and $5d6p\ ^3P_J^o$ states give very small collisional deactivation cross sections. This implies that the Ba($5d6p$)-He potential curves, which are asymptotically correlated to $^1P_1^o$ and $^3P_J^o$, respectively, do not have effective crossings. This is different from the cases for $6s6p$ and $6s5d$, where singlet-triplet mixing of $6s6p\ ^1P_1^o$–$^3P_2^o$ and $6s5d\ ^1D_2$–$^3D_3$ have been observed [16,22]. A small deactivation cross section for $5d6p\ ^1F_3^o$ may suggest the absence of effective potential crossing with nearby levels. Second,

upper two states of $5d6p\ ^3D_J^o$ give similar deactivation cross sections, which indicates nearly identical collisional processes for the two states. Although we are not yet able to make a definitive statement only from the deactivation cross sections, our preliminary result on the state-to-state cross sections among $5d6p\ ^3D_J^o$ suggests that fine-structure mixing is dominated by intermultiplet mixing (with $5d6p\ ^3F_J^o$) and mixing with different electron configuration ($5d^2\ ^3P_J$) [33]. The $5d6p\ ^3D_J^o$ states seem to follow the general propensity rule that fine-structure mixing is relatively small. Finally, large deactivation cross sections are obtained for the $5d6p\ ^3F_{3,4}^o$ and $^1D_2^o$ states. Since the energy levels around $5d6p\ ^3F_J^o$ are congested, it is difficult to conclude whether these large deactivation cross sections arise from fine-structure mixing among $^3F_J^o$ or level crossing with other multiplets and electronic configurations. Nevertheless, high state density in the 22 000–24 000 cm^{-1} region is considered to be the origin of the fast deactivation of those states according to the general propensity rule. For the $5d6p\ ^3F_2^o$ state, couplings with the $5d^2\ ^3F_3$ and $6s6p\ ^1P_1$ states are expected from the theoretical potential curves [32]. A relatively small deactivation cross section of the $5d6p\ ^3F_2^o$ state suggests that these couplings are not as strong as those of the $5d6p\ ^3F_{3,4}^o$ and $^1D_2^o$ states.

For the $5d^2\ ^3P_2$ state, slow radiative decay is observed compared with the nearby $5d6p$ states while collisional decay appears as fast as that of the congested $5d6p$ states around $^3F_J^o$. Unfortunately, we could not observe sensitized fluorescence from the other $5d^2$ states because the photomultiplier tube used in the experiment does not have sensitivity in the longer wavelength region (>900 nm).

For a more detailed discussion of a collision-induced transition of Ba in doubly excited states, we need to wait for the development of a theoretical study of the Ba($5d6p$)-He and Ba($5d^2$)-He systems as well as experimental investigation of state-to-state cross sections. Further analysis of time-resolved sensitized fluorescence signals for the $5d6p$ and nearby states is now in progress [33].

V. CONCLUSIONS

We have developed a technique to produce Ba atoms in the $6s5d\ ^3D_J$ metastable states by laser ablation of a solid Ba sample in vacuum and He buffer gas at room temperature, and measured radiative lifetimes and collisional deactivation cross sections of the $5d6p$ states. Barium atoms in the $6s5d\ ^3D_J$ metastable states are excited to the $5d6p$ states by a pulsed dye laser. Radiative lifetimes and collisional deactivation cross sections with He gas are obtained for the upper states by analyzing the time profiles of LIF. Radiative lifetimes of the $5d6p\ ^3P_J^o$, $^3D_J^o$, and $^3F_J^o$ states do not show clear *J*-dependence, suggesting the validity of LS coupling. Collisional deactivation with He is relatively fast for the $5d6p\ ^3D_J^o$, $^1D_2^o$, $^3F_{3,4}^o$ states, whereas deactivation of the $5d6p\ ^3P_J^o$, $^1P_1^o$, $^3F_2^o$, and $^1F_3^o$ states is much slower in the He pressure range of 60–400 Pa. It is considered that collisional fine-structure mixing is small for the $5d6p$ states compared with intermultiplet mixing. When Ba atoms are excited to the $5d6p\ ^3D_1^o$ state, we have observed sensitized fluorescence from the $5d^2\ ^3P_2$ state, which is collisionally populated from the laser-excited state. Radiative lifetime and collisional deactivation cross section are determined for the $5d^2\ ^3P_2$ state from the pressure dependence of decay rates of the sensitized fluorescence. Radiative lifetime of the $5d^2\ ^3P_2$ state is long compared with nearby $5d6p$ states, while deactivation cross section is comparable to those of the congested $5d6p$ states around $^3F_J^o$.

ACKNOWLEDGMENTS

One of us (T.N.) acknowledges support from the Special Researcher's Basic Science Program of RIKEN. This work was supported by the President's Special Research Grant from The Institute of Physical and Chemical Research (RIKEN).

[1] B. M. Miles and W. L. Wiese, At. Data **1**, 1 (1969).
[2] L. O. Dickie and F. M. Kelly, Can. J. Phys. **48**, 879 (1970); **49**, 1098 (1971); **49**, 2630 (1971).
[3] J. Brecht, J. Kowalski, G. Lidö, I. -J. Ma, and G. zu Putlitz, Z. Phys. **264**, 273 (1973).
[4] K. Ueda, Y. Hamaguchi, T. Fujimoto, and K. Fukuda, J. Phys. Soc. Jpn. **53**, 2501 (1984).
[5] M. Aymar, R. -J. Champeau, C. Delsart, and J. -C. Keller, J. Phys. B **14**, 4489 (1981).
[6] M. Aymar, P. Grafstrom, C. Levison, H. Lundberd, and S. Svanberg, J. Phys. B **15**, 877 (1982).
[7] L. Jahreiss and M. C. E. Huber, Phys. Rev. A **31**, 692 (1985).
[8] S. Niggli and M. C. E. Huber, Phys. Rev. A **35**, 2908 (1987).
[9] S. Niggli and M. C. E. Huber, Phys. Rev. A **39**, 3924 (1989).
[10] G. Garucía and J. Campos, J. Quant. Spectrosc. Radiat. Transf. **42**, 567 (1989).
[11] A. Bizzarri and M. C. E. Huber, Phys. Rev. A **42**, 5422 (1990).
[12] P. E. Jessop and F. M. Pipkin, Phys. Rev. A **20**, 269 (1979).
[13] G. Brink, A. Glassman, and R. Gupta, Opt. Commun. **33**, 17 (1980).
[14] J. E. Smedley and D. F. Marran, Phys. Rev. A **47**, 126 (1993).
[15] J. L. Bowen and A. P. Thorne, J. Phys. B **18**, 35 (1985).
[16] W. H. Breckenridge and C. N. Merrow, J. Chem. Phys. **88**, 2329 (1988).
[17] A. Kallenbach and M. Kock, J. Phys. B **22**, 1795 (1989).
[18] J. P. Visticot, J. Berlande, J. Cuvellier, J. M. Mestdagh, P. Meynadier, P. de Pujo, O. Sublemontier, A. J. Bell, and J. G. Frey, J. Chem. Phys. **93**, 5354 (1990).
[19] E. Ehrlacher and J. Huennekens, Phys. Rev. A **46**, 2642 (1992).
[20] E. Ehrlacher and J. Huennekens, Phys. Rev. A **50**, 4786 (1994).
[21] C. Vadla, K. Niemax, V. Horvatic, and R. Beuc, Z. Phys. D **34**, 171 (1995).

[22] J. Brust and A. C. Gallagher, Phys. Rev. A **52**, 2120 (1995), and references on alkali-earth atoms Mg, Ca, and Sr are also therein.
[23] J. E. Smedley, D. F. Marran, M. R. Peabody, and C. N. Marquis, J. Chem. Phys. **98**, 1093 (1993).
[24] T. Nakajima, Y. Matsuo, and M. Takami, Phys. Scr. **56**, 599 (1997).
[25] N. Yonekura, T. Nakajima, Q. Hui, and M. Takami, Chem. Phys. Lett. **280**, 525 (1997).
[26] Y. Matsuo, T. Nakajima, T. Kobayashi, and M. Takami, Appl. Phys. Lett. **71**, 996 (1997).
[27] T. Nakajima, Y. Matsuo, N. Yonekura, M. Nakamura, and M. Takami, J. Phys. B **31**, 1729 (1998).
[28] T. Nakajima, N. Yonekura, Y. Matsuo, Q. Hui, and M. Takami, Phys. Rev. A **57**, 3598 (1998).
[29] J. Migdalek and W. E. Baylis, Phys. Rev. A **42**, 6897 (1990).
[30] A. Hermanni and G. Werth, Z. Phys. D **11**, 301 (1989).
[31] R. Ladenburg, Rev. Mod. Phys. **5**, 243 (1933).
[32] J. Brust and C. H. Greene, Phys. Rev. A **56**, 2005 (1997); **56**, 2013 (1997).
[33] Y. Matsuo, T. Nakajima, T. Kobayashi, and M. Takami (unpublished).